Crystal structure of the Nogo-Receptor-2

Mariya Semavina,[1] Nayanendu Saha,[1] Momchil V. Kolev,[1] Yehuda Goldgur,[1] Roman J. Giger,[2] Juha P. Himanen,[1] and Dimitar B. Nikolov[1]*

[1]Structural Biology Program, Memorial Sloan Kettering Cancer Center, 1275 York Avenue, New York 10065
[2]Departments of Cell and Developmental Biology and Neurology, University of Michigan School of Medicine, The University of Michigan, Ann Arbor, Michigan 48109

Received 19 November 2010; Accepted 18 January 2011
DOI: 10.1002/pro.597
Published online 24 January 2011 proteinscience.org

Abstract: The inhibition of axon regeneration upon mechanical injury is dependent on interactions between Nogo receptors (NgRs) and their myelin-derived ligands. NgRs are composed of a leucine-rich repeat (LRR) region, thought to be structurally similar among the different isoforms of the receptor, and a divergent "stalk" region. It has been shown by others that the LRR and stalk regions of NgR1 and NgR2 have distinct roles in conferring binding affinity to the myelin associated glycoprotein (MAG) *in vivo*. Here, we show that purified recombinant full length NgR1 and NgR2 maintain significantly higher binding affinity for purified MAG as compared to the isolated LRR region of either NgR1 or NgR2. We also present the crystal structure of the LRR and part of the stalk regions of NgR2 and compare it to the previously reported NgR1 structure with respect to the distinct signaling properties of the two receptor isoforms.

Keywords: nogo receptor; X-ray crystallography; glycosylation; ligand binding

Introduction

The ability of the adult central nervous system to regenerate after injury is very limited due to the formation of a glial scar[1–4] and the presence of inhibitory molecules in the myelin debris.[5–8] The myelin-associated glycoprotein (MAG),[9,10] Nogo-A and the olygodendrocyte myelin glycoprotein (OMgp) repress axon regeneration after mechanical damage. These myelin-derived inhibitors share no amino acid sequence or domain similarity; however, they bind to the same neuronal receptor, which was initially identified as a receptor for Nogo-A and termed NgR.[11] It was later confirmed that NgR binds MAG and OMgp as well.[12–15] As a glycosylphosphatidylinositol (GPI)-anchored receptor, NgR lacks both the transmembrane and the intracellular domains. A number of possible signal transducing partners of NgR have been identified, which include p75,[16,17] LINGO,[18] and TROY.[19,20] The complex cascade of reactions occurring upon receptor complex formation culminates in changes in the neuronal cytoskeleton that manifests in collapse of the neuronal growth cone.

In addition to NgR1, two other isoforms of the receptor, NgR2 and NgR3, were identified based on amino acid sequence similarity and biochemical homology.[21–25] NgRs belong to the family of leucine-rich repeat (LRR) proteins. Nogo receptors contain eight LRRs flanked by the N- and C-terminal cysteine-rich regions (LRRNT and LRRCT, respectively), typical of this family of proteins.[26] This N-terminal region is highly conserved at the amino acid sequence level among the NgRs. The LRR domain is connected to the GPI-anchor for membrane attachment via a C-terminal "stalk" region. The stalk sequence is more divergent among the NgRs; there are no defined structural motifs that can be predicted based on its amino acid composition. However, the importance of this region has been clearly illustrated in studies of the receptor binding to MAG and Nogo-66 *in vivo*.[25,27] The stalk region could also be involved in the interactions of the Nogo receptors with co-receptors such as LINGO1 (unpublished observation). The crystal structure of the LRR domain of human NgR1 has been determined previously.[21,28]

Grant sponsor: The New York State Spinal Cord Injury Research Program; Grant number: C-022047; Grant sponsor: RO1; Grant number: NIH/NINDS NS047333

**Correspondence to:* Dimitar B. Nikolov, Structural Biology Program, Memorial Sloan Kettering Cancer Center, 1275 York Avenue, NY 10065. E-mail: nikolovd@mskcc.org

Table I. *Summary of Crystallographic Data*

	NgR2-310	NgR2-330
Space group	$P2_12_12_1$	$P2_12_12_1$
Unit cell dimensions (Å)	$a = 56.8$, $b = 56.5$, $c = 28.9$	$a = 56.8$, $b = 129.1$, $c = 57$
Resolution (Å)[a]	25.0 – 1.8 (1.9–1.8)	25.0 – 2.1 (2.2–2.1)
Completeness (%)	97.3 (76.9)	98.6 (89.5)
Number of reflections	38016	23662
R_{merge} (%)[b]	10.4 (41.2)	13.1 (44.2)
I/σ_I	18.3 (2.9)	19.4 (2.6)
R_{factor} (%)[c]	17.1 (28.6)	16.4 (22.6)
R_{free} (%)[c]	20.5 (37.3)	19.8 (30.6)
No. of nonhydrogen atoms	2684	2645
No. of waters	365	298
rmsd bonds (Å)	0.031	0.027
rmsd angles (°)	2.413	2.078

Each dataset was collected from a single crystal. Data statistics treats Bijvoët mates independently.
[a] Values in parentheses correspond to the high resolution shell.
[b] $R_{merge} = \sum|I - \langle I\rangle|/\sum I$, where I is the observed intensity and $\langle I\rangle$ is the statistically weighted absolute intensity of multiple measurements of symmetry related reflections. The values in brackets are for the highest resolution shell.
[c] $R = \sum||F_o| - k|F_c||/\sum|F_o|$, R_{factor} from the working set and R_{free} from the test set

Here, we report two structures of NgR2, one includes the LRR domain only and the other the LRR domain and part of the stalk region.

Results

We crystallized NgR2 (27-310), which contains the LRR repeats and the flanking cysteine-rich domains (LRRNT and LRRCT), and a slightly longer version, NgR2 (27-330), which includes a part of the stalk domain. However, the region beyond residue 315 is disordered in the electron density map of NgR2-330 and was not modeled in the final structure. The NgR2-310 and NgR2-330 crystals diffracted to 1.8 Å and 2.1 Å, respectively, and the structure refinement statistics are summarized in Table I. Our attempts to obtain crystals of the full length NgR2 were unsuccessful partly due to protein instability (fast degradation). Human NgR1 and rat NgR2 share 50% amino acid sequence identity in the described region (residues 27–330). Consequently, our NgR2-310 structure is overall very similar to that of NgR1-311 with the RMSD of 0.69 Å between 251 Cα atoms [Fig. 1(A)]. The molecular architecture of the two NgR2 constructs is that of a typical LRR with eight repeating segments, each comprised of a short β-strand and an extended loop. The arrangement of β-strands and loops in LRR NgR2 is very similar to that in NgR1 with the exception of a short α-helix composed of residues Thr101-Arg103 present in NgR2, but not in NgR1 [arrow 1 in Fig. 1(A)].

Similar to their NgR1 counterparts, the LRR capping regions of NgR2 are stabilized by four disulfide bonds: Cys31-Cys37, Cys35-Cys46 at the N-terminus and Cys265-Cys287, Cys267-Cys310 at the C-terminus. Interestingly, there is also a free cysteine buried inside the protein structure at the position 141. The LRRNT of NgR2 forms a loop between two short β-strands (residues Thr36-Thr38 and Thr43-Ser45). In contrast, this region in NgR1 does not adopt a defined secondary structure and is one amino acid longer than in NgR2 [arrow 2 in Fig. 1(A)]. The region comprising amino acids 104–243 is structurally identical in the two proteins. The differences between NgR1 and NgR2 are localized to the LRRCT capping region: there is a short α-helix formed by Gly244-Asp249 in NgR2, but not in NgR1. In addition, the α-helix that spans Asp297-Leu306 in NgR1 is split into two shorter helices (Leu299-Thr301 and Asp304-Gln308) in NgR2, possibly providing a basis for more flexibility in the adjacent stalk region.

Interestingly, the glycosylation pattern in NgR2 differs significantly from that of NgR1. In the previously reported structures of NgR1[21,28] the two glycosylation sites are Asn82 and Asn179 [Fig. 1(C)], whereas in our structure of NgR2 these asparagine residues (structurally corresponding residues are Asn83 and Asn180, of which only Asn180 has a potential for sugar attachment) are not glycosylated. Instead, Asn50, Asn93, and Asn236 are glycosylated in NgR2 [Fig. 1(D)], while in NgR1 nonpolar residues are found at these positions. Thus, in our structure three out of four potential sites are glycosylated. This important difference can contribute to the distinct ligand binding preferences of NgR1 versus NgR2.

Similarly to NgR1, the LRR of NgR2 carries an overall positive charge with a theoretical pI of 9. In contrast, the stalk region at physiological pH has opposite charges in the two proteins: the calculated pI of the stalk in NgR1 and NgR2 is 9 and 5, respectively. Positive and negative charges on the surface of NgR2 form several compact patches (Fig. 2). A distinctive feature of this charge distribution is the large S-shaped negatively charged area on the convex surface, which extends into the beginning of the

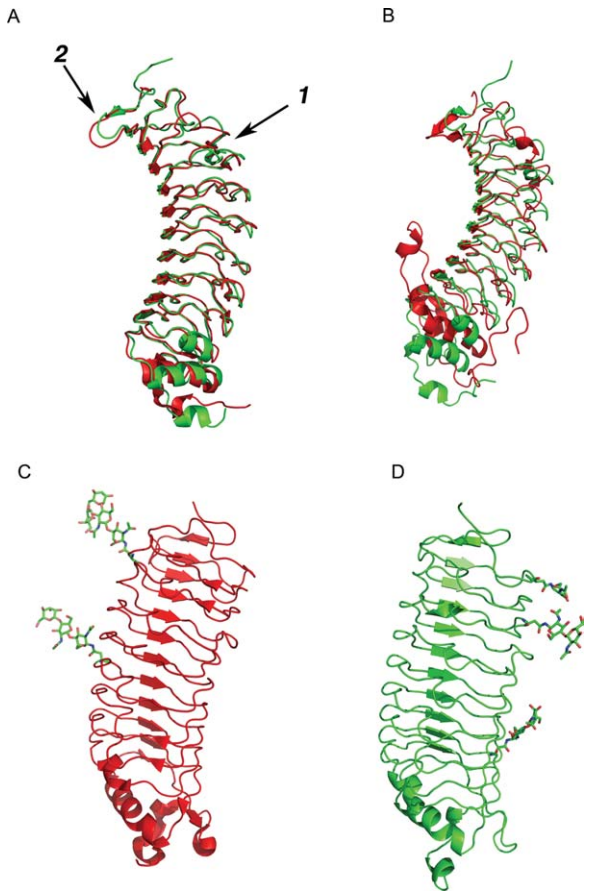

Figure 1. Structure of NgR2. (A) Comparison of the structure of NgR1-311 (red) and NgR2-310 (green). Arrows point to the differences between NgR1 and NgR2. (B) Superposition of NgR2 (330) (green) and GpIbα (red). (C) Structure of NgR1 (311) with Asn-linked glycosylation shown as bonds. (D) Structure of NgR2-330 with Asn-linked glycosylation shown as bonds. Molecules in (C) and (D) are in similar orientation.

stalk region (arrows 1 and 2 in Fig. 2). The corresponding area is much smaller in NgR1 (bottom panel in Fig. 2). Parallel to the acidic region is a band of positively charged residues in NgR2, while in NgR1 this area is mostly neutral. Two acidic regions are found on the side of NgR2 (arrows 3 and 4) with positively charged residues localized to the opposite side and the concave surface of the protein (arrows 5 and 6).

To characterize the MAG interaction with the NgR LRR domain as compared to that with the full-length NgR1 and NgR2 proteins we used ELISA-based *in vitro* binding assays. Our data clearly show that the presence of the stalk region greatly enhances receptor binding to MAG (Fig. 3) for both NgR1 and NgR2, when using recombinant purified proteins.

Discussion

Recent findings have alluded to the fact that the LRR and stalk regions of the Nogo receptors have distinct roles in the interactions of these receptors with their ligand MAG. In particular, the NgR2 LRRCT+stalk region, alone or when fused to the LRR of either NgR1 or NgR2, appears to significantly enhance receptor binding to MAG *in vivo*.[25,27] The exact role of the stalk region is not well understood, however, partly due to the lack of structural information. The purpose of this study was to determine the structure of NgR2 to further our understanding of the distinct ligand-binding affinities and specificities of the different members of this receptor family.

We crystallized two different NgR2 constructs: NgR2 (27-310) and NgR2 (27-330) (Table I). The crystal structures revealed that the overall architecture of the LRR region of NgR2 is very similar to that of NgR1. The major structural differences are located at the C-terminus of the LRRCT region. The distances between corresponding α-carbons in this region progressively increase (2.9 Å for residue 304, 3.4 Å for residue 310, 8.3 Å for residue 311), implying that the adjacent stalk region of NgR2 is also structurally different from that of NgR1. Our structures suggest that the two short α-helices in the beginning of the stalk region of NgR2 (as opposed to one longer helix in NgR1) may render the stalk region more flexible than in NgR1, which would affect ligand-induced structural rearrangements and, consequently, binding affinity. We were unable to obtain any structural data on most of the stalk region as longer versions of NgR2 failed to crystallize and this region was mostly disordered in our NgR2 (27-330) crystals, confirming that the stalk is disordered in the unbound form of the receptor. Low degree of conservation in the amino acid composition of the stalk region between the NgR homologs may partly explain the difference in their binding affinity to MAG. In addition, different charge distributions within the LRRs of the NgRs may affect NgR-MAG interactions indirectly. Specifically, the continuous positively charged area on both the convex and concave sides of NgR2 can contribute to binding of the negatively-charged MAG (theoretical pI = 4.8) under physiological conditions.

The large surface area of the NgR isoforms provide an extensive platform for binding a diverse group of ligands.[21] Indeed, the different binding partners of the Nogo receptors share neither amino acid sequence similarity nor structural domain organization. Similar protein surface utilization for binding structurally very different ligands is illustrated by the LRR-containing glycoprotein GpIbα and its complexes.[29,30] Strikingly, our NgR2 (27-330) structure can be superimposed on the structure of glycoprotein GpIbα with the RMSD of 1.6 Å [Fig. 1(B)]. The major differences between the two structures are localized to their C-terminal regions. The LRRCT region of GpIbα forms a β-switch on the

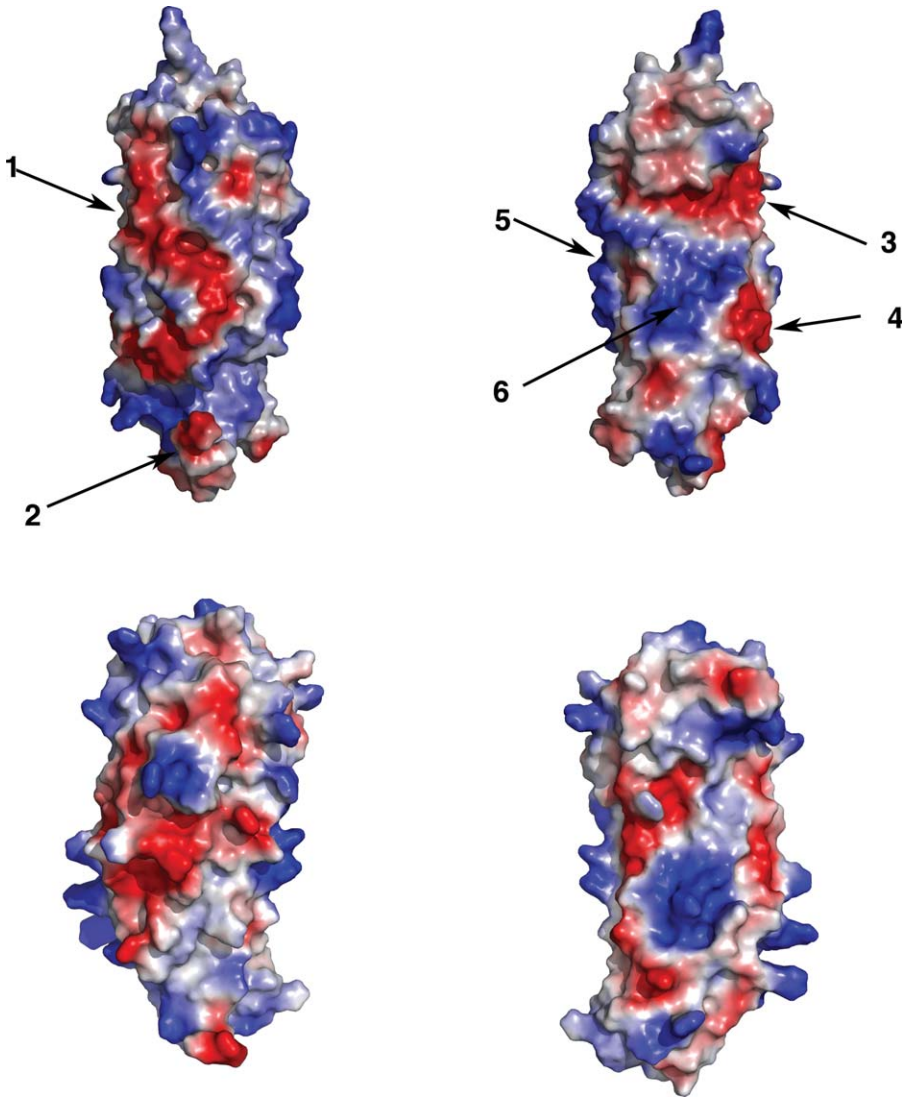

Figure 2. The molecular surface of NgR2 (330) (top) and NgR1 (311) (bottom) colored according to their electrostatic potential. Convex (left) and concave (right) surfaces are shown. Red indicates negative charge and blue indicates positive charge.

concave surface, a feature important for protein function: it folds into a β-hairpin upon binding to von Willebrand factor (VWF), stabilizing the contact areas between the two proteins;[29] NgR2 lacks this structural feature. In addition, the extended LRRCT of GpIbα folds onto the convex side of the molecule in the unliganded state, and moves away as part of structural rearrangements occurring upon biding to thrombin.[30] Thus, the two proteins (VWF and thrombin) bind to opposite sides of the GpIbα molecule. It is unclear whether the Nogo receptors bind their various ligands in a structurally similar fashion, and further studies are required to define the exact roles of the different surface regions of the Nogo receptors in binding their various ligands.

Finally, our structure clearly points to the major difference between the two NgR isoforms – the glycosylation patterns in the LRR region. Since this profound difference in the molecular surface properties cannot be attributed to the different protein expression systems used in NgR1 and NgR2 structural studies (here we used insect cells whereas both insect and mammalian cells were used in the reported NgR1 structures), we propose that the differences in receptor glycosylation might be the main reason for the different ligand binding and signaling properties of NgR1 versus NgR2.

Materials and Methods

Protein expression and purification

DNA fragment encoding amino acids 27–310 (LRRNT + LRR + LRRCT) and 27–330 were amplified by PCR from the rat full-length NgR2 clone in a pMT21 vector. Each fragment, including the N-terminal signal sequence, and fused C-terminally to the Fc region if human IgG, was cloned into the BamHI and EcoRI sites of the pMA-152a baculovirus vector.

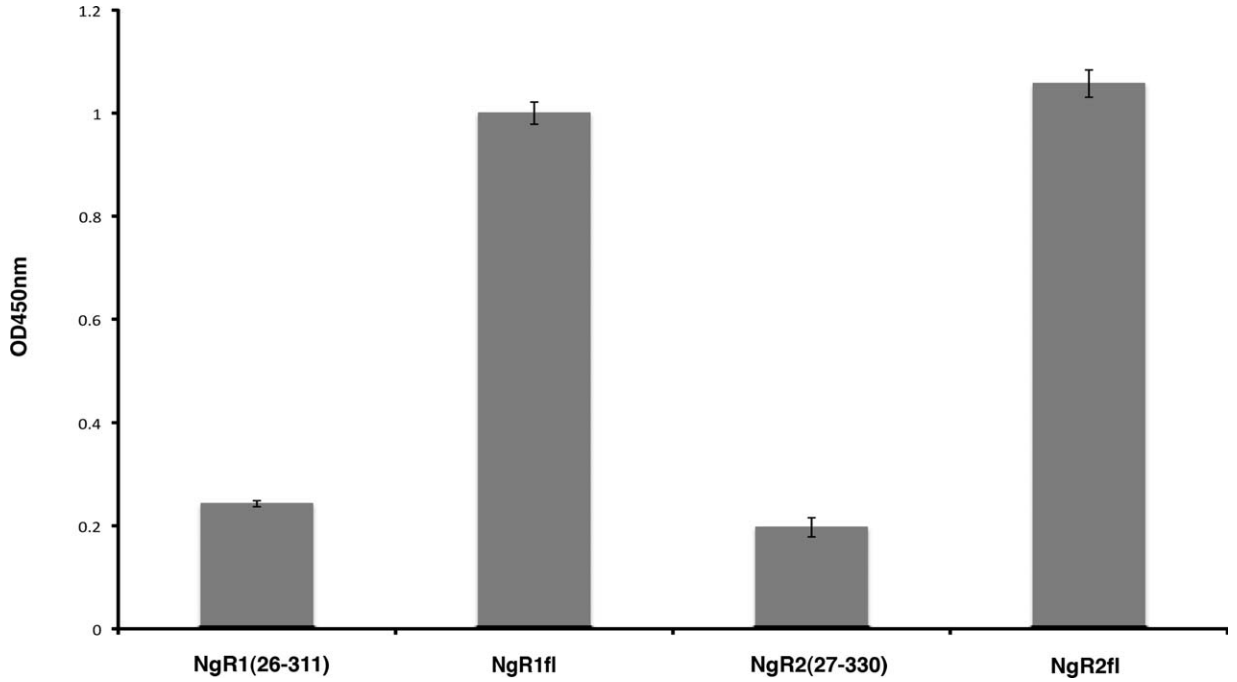

Figure 3. Comparison of the MAG binding affinities of the isolated LRR domains with that of the full-length NgR1 and NgR2 proteins. Data were corrected for Fc fragment binding to immobilized MAG and normalized with respect to full-length NgR1. Error bars represent the s.d. of four independent measurements and "fl" refers to full-length.

The vector was then transfected into Sf9 cells. Passage 3 recombinant virus was used for Hi5 cells infection in SF-900 II serum-free medium. The cells were grown in suspension at 27°C and 100 rpm. The protein was purified from expression medium using protein-A sepharose chromatography followed by removal of the Fc tag by thrombin and gel-filtration chromatography. The apparent molecular mass of each protein was ~40 kDa, higher than the calculated mass of 32 kDa due to glycosylation. NgR2 (27-310) and NgR2 (27-330) were purified to >95% purity as indicated by SDS-PAGE.

Crystallization and structure determination

Purified protein was concentrated to 10 mg/mL in 10 m*M* HEPES (pH 7.2) and 500 m*M* KCl and crystallized at 20°C in a hanging drop containing equal volumes of protein and well solution. The well solution for NgR2 (310) contained 100 m*M* HEPES-Na (pH 7.5), 10% isopropanol, and 15% polyethylene glycol 10,000, for NgR2 (330)–or 0.6*M* K/$NaPO_4$, pH 7.6. For structure determination single-wavelength data sets were collected at Advanced Photon Source beamline ID-24. The structures were determined by molecular replacement with NgR1 (26-311) as a model (see Table I).

Binding assays

Wells of a 96-well microtiter plate (Nunc) were coated overnight at 4°C with 2 μg of purified MAG in 0.1 mL of buffer (10 m*M* HEPES, 150 m*M* KCl, 0.05% Tween 20 at pH 7.4). Unbound protein was decanted and the wells washed thrice with the same buffer. They were then filed with 0.2 mL of 2% nonfat milk (Bio-Rad) and incubated at 25°C for 1 hour. The wells were washed again and incubated in quadruplicate with 1 μg of either NgR1 (26-311)-Fc, NgR1 (26-460)-Fc, NgR2 (27-330)-Fc, or NgR2 (27-420)-Fc for 1 hour at 25°C. Purified Fc fragment was used as a control. After washing, the wells were incubated for 1 hour with 0.1 mL of affinity-pure goat anti-human IgG, Fc fragment specific antibody (Jackson immuno research laboratory) at a dilution of 1:200. After washing, the wells were incubated with donkey anti-goat IgG conjugated to horseradish peroxidase (Promega) at a dilution of 1:2000 for 1 hour. Finally, color was developed using the immunopure TMB substrate kit (Thermoscientific) and OD at 450 nm was recorded on a 96-well plate reader Victor X5 (Perkin Elmer). Data points were corrected for the binding of the isolated Fc fragment to MAG and normalized with respect to full-length NgR1.

References

1. Rudge J, Silver J (1990) Inhibition of neurite outgrowth on astroglial scars in vitro. J Neurosci 10: 3594–3603.
2. Snow DM, Steindler DA, Silver J (1990) Molecular and cellular characterization of the glial roof plate of the spinal cord and optic tectum: a possible role for a proteoglycan in the development of an axon barrier. Dev Biol 138:359–376.
3. McKeon R, Schreiber R, Rudge J, Silver J (1991) Reduction of neurite outgrowth in a model of glial scarring following CNS injury is correlated with the

expression of inhibitory molecules on reactive astrocytes. J Neurosci 11:3398–3411.
4. Ferretti P, Zhang F, O'Neill P (2003) Changes in spinal cord regenerative ability through phylogenesis and development: lessons to be learnt. Dev Dynam 226: 245–256.
5. Ramon y Cajal S (1928) Degeneration and regeneration of the nervous system. Oxford, UK: Oxford University Press.
6. Schwab ME, Kapfhammer JP, Bandtlow CE (1993) Inhibitors of neurite growth. Annu Rev Neurosci 16: 565–595.
7. Filbin MT (2003) Myelin-associated inhibitors of axonal regeneration in the adult mammalian CNS. Nat Rev Neurosci 4:703–713.
8. McGee AW, Strittmatter SM (2003) The Nogo-66 receptor: focusing myelin inhibition of axon regeneration. Trends Neurosci 26:193–198.
9. McKerracher L, David S, Jackson DL, Kottis V, Dunn RJ, Braun PE (1994) Identification of myelin-associated glycoprotein as a major myelin-derived inhibitor of neurite growth. Neuron 13:805–811.
10. Mukhopadhyay G, Doherty P, Walsh FS, Crocker PR, Filbin MT (1994) A novel role for myelin-associated glycoprotein as an inhibitor of axonal regeneration. Neuron 13:757–767.
11. Fournier AE, GrandPre T, Strittmatter SM (2001) Identification of a receptor mediating Nogo-66 inhibition of axonal regeneration. Nature 409:341–346.
12. Domeniconi M, Cao Z, Spencer T, Sivasankaran R, Wang KC, Nikulina E, Kimura N, Cai H, Deng K, Gao Y, He Z, Filbin M (2002) Myelin-associated glycoprotein interacts with the Nogo66 receptor to inhibit neurite outgrowth. Neuron 35:283–290.
13. Kottis V, Thibault P, Mikol D, Xiao Z-C, Zhang R, Dergham P, Braun PE (2002) Oligodendrocyte-myelin glycoprotein (OMgp) is an inhibitor of neurite outgrowth. J Neurochem 82:1566–1569.
14. Liu BP, Fournier A, GrandPre T, Strittmatter SM (2002) Myelin-associated glycoprotein as a functional ligand for the Nogo-66 receptor. Science 297:1190–1193.
15. Wang KC, Koprivica V, Kim JA, Sivasankaran R, Guo Y, Neve RL, He Z (2002) Oligodendrocyte-myelin glycoprotein is a Nogo receptor ligand that inhibits neurite outgrowth. Nature 417:941–944.
16. Wang KC, Kim JA, Sivasankaran R, Segal R, He Z (2002) p75 interacts with the Nogo receptor as a co-receptor for Nogo, MAG and OMgp. Nature 420:74–78.
17. Wong ST, Henley JR, Kanning KC, Huang K-h, Bothwell M, Poo M-m (2002) A p75NTR and Nogo receptor complex mediates repulsive signaling by myelin-associated glycoprotein. Nat Neurosci 5:1302–1308.
18. Mi S, Lee X, Shao Z, Thill G, Ji B, Relton J, Levesque M, Allaire N, Perrin S, Sands B, Crowell T, Cate RL, McCoy JM, Pepinsky RB (2004) LINGO-1 is a component of the Nogo-66 receptor/p75 signaling complex. Nat Neurosci 7:221–228.
19. Park JB, Yiu G, Kaneko S, Wang J, Chang J, He Z (2005) A TNF receptor family member, TROY, is a coreceptor with Nogo receptor in mediating the inhibitory activity of myelin inhibitors. Neuron 45:345–351.
20. Shao Z, Browning JL, Lee X, Scott ML, Shulga-Morskaya S, Allaire N, Thill G, Levesque M, Sah D, McCoy JM, Murray B, Jung V, Pepinsky RB, Mi S (2005) TAJ/TROY, an orphan TNF receptor family member, binds Nogo-66 receptor 1 and regulates axonal regeneration. Neuron 45:353–359.
21. Barton WA, Liu BP, Tzvetkova D, Jeffrey PD, Fournier AE, Sah D, Cate R, Strittmatter SM, Nikolov DB (2003) Structure and axon outgrowth inhibitor binding of the Nogo-66 receptor and related proteins. EMBO J 22:3291–3302.
22. Lauren J, Airaksinen MS, Saarma M, Timmusk T (2003) Two novel mammalian nogo receptor homologs differentially expressed in the central and peripheral nervous systems. Mol Cell Neurosci 24:581–594.
23. Pignot V, Hein AE, Barske C, Wiessner C, Walmsley AR, Kaupmann K, Mayeur H, Sommer B, Mir AK, Frentzel S (2003) Characterization of two novel proteins, NgRH1 and NgRH2, structurally and biochemically homologous to the Nogo-66 receptor. J Neurochem 85:717–728.
24. Klinger M, Taylor JS, Oertle T, Schwab ME, Stuermer CAO, Diekmann H (2004) Identification of Nogo-66 receptor (NgR) and homologous genes in fish. Mol Biol Evol 21:76–85.
25. Venkatesh K, Chivatakarn O, Lee H, Joshi PS, Kantor DB, Newman BA, Mage R, Rader C, Giger RJ (2005) The Nogo-66 receptor homolog NgR2 is a sialic acid-dependent receptor selective for myelin-associated glycoprotein. J Neurosci 25:808–822.
26. Kobe B, Kajava AV (2001) The leucine-rich repeat as a protein recognition motif. Curr Opin Struct Biol 11: 725–732.
27. Robak LA, Venkatesh K, Lee H, Raiker SJ, Duan Y, Lee-Osbourne J, Hofer T, Mage RG, Rader C, Giger RJ (2009) Molecular basis of the interactions of the Nogo-66 receptor and its homolog NgR2 with myelin-associated glycoprotein: development of NgROMNI-Fc, a novel antagonist of CNS myelin inhibition. J Neurosci 29:5768–5783.
28. He XL, Bazan JF, McDermott G, Park JB, Wang K, Tessier-Lavigne M, He Z, Garcia KC (2003) Structure of the Nogo receptor ectodomain: a recognition module implicated in myelin inhibition. Neuron 38:177–185.
29. Huizinga EG, Tsuji S, Romijn RAP, Schiphorst ME, de Groot PG, Sixma JJ, Gros P (2002) Structures of Glycoprotein Ibalpha and Its Complex with von Willebrand Factor A1 Domain. Science 297:1176–1179.
30. Dumas JJ, Kumar R, Seehra J, Somers WS, Mosyak L (2003) Crystal structure of the GpIb{alpha}-thrombin complex essential for platelet aggregation. Science 301: 222–226.